ISBN: 978-3-95450-184-7 doi:10.18429/JACoW-IPAC2018-THPAK001

IMPEDANCE EVALUATION OF IN-VACUUM UNDULATOR AT KEK PHOTON FACTORY

O. Tanaka†, N. Nakamura, T. Obina, K. Tsuchiya, R. Takai, S. Sakanaka, N. Yamamoto, R. Kato, M. Adachi, High Energy Accelerator Research Organization (KEK), Tsukuba, Japan

Abstract

The estimate of impedance and kick factors of the recently installed at KEK Photon Factory (PF) four In-Vacuum Undulators (IVU) is currently a very important issue, because they could be considerable contributors to the total impedance of PF. Moreover, the coupling impedance of the IVUs could lead to the beam energy loss, changes in the bunch shape, betatron tune shifts and, finally, to the various beam instabilities. Using the simulation tool (CST Particle Studio), longitudinal and transverse impedances of the IVUs were evaluated and compared to analytical formulas and measurement results. The study provides guidelines for mitigation of unwanted impedance, for the accurate estimate of its effects on the beam quality and beam instabilities and also for the impedance budget of a newly designed next-generation machine which has many IVUs and small-aperture beam pipes.

INTRODUCTION

At KEK Photon Factory (PF) light source, we have four newly installed In-Vacuum Undulators (IVUs). The IVU's vacuum chamber has a complex geometry. It consists of two taper transitions between the undulator and the beam chamber, two copper plates on the undulator magnets for RF shielding of the magnets from a beam, and two step transitions between the octagon and the taper region. Each part makes its own impact on the total frequency dependent impedance of the entire IVU. Design issues of IVU including taper regions, undulator plates and step transitions are well-studied (see, for example, [1] – [4]).

To quantify IVUs induced impedance we engaged both a powerful simulation tool (Wakefield Solver of CST Particle Studio [5]), and theoretical assessments (for cross-checking the results of simulation), and, finally, an experimental reconciliation of the impedance values obtained from our studies. Such a comprehensive analysis shown in this article will be a standard procedure for the design of new accelerators. It allows to predict the thresholds of instabilities and to assess the influence of collective effects [6] – [7].

This study shows how we identify the major impedance contributors and evaluate their impedance using theoretical formulas, CST Studio simulations and measurements. Now, let us discuss in details these impedance evaluations, and its experimental confirmation.

IMPEDANCE EVALUATION FOR PF IVU BY SIMULATIONS AND THEORY

PF IVU consists of three parts (see Fig. 1 a) – c)). Each of these parts impacts into the total impedance of the IVU.

† olga@post.kek.jp

- Taper between the flange and the undulator (200 mm thick) for the geometrical impedance.
- Copper plate (60 mm copper and 25 mm nickel coating) on top of the undulator for the resistive-wall impedance.
- Step transition from the octagon to the rectangular chambers.

In the following each contributor will be treated separately.

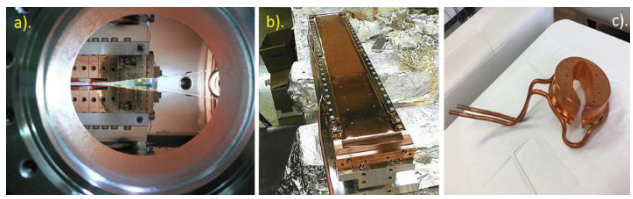

Figure 1: Three major impedance contributors of PF IVU: a). Taper between the flange and the undulator; b). Copper plate on top of the undulator; c). Step transition from the octagon to the rectangular chambers.

Geometrical Impedance of Taper

To calculate the pure geometrical impedance of the taper, we first assume the perfectly conductive material instead of using copper resistivity. The CST model of the taper is shown at Fig. 2.

The taper structure is known to produce nearly pure inductive impedance even with a vessel included. The theoretical formula for the normalized longitudinal impedance reads [8] (see Fig. 3):

$$\frac{Z_l}{n} = -i\frac{Z_0\omega_0}{4\pi c}\int_{-\infty}^{\infty}(g')^2 F\left(\frac{g}{w}\right)dz, \qquad (1)$$

$$F(x) = \sum_{m=0}^{\infty}\frac{1}{2m+1}\operatorname{sech}^2\left((2m+1)\frac{\pi x}{2}\right)\tanh\left((2m+1)\frac{\pi x}{2}\right). \qquad (2)$$

Here $Z_0 = 377\Omega$ is the impedance of the free space, and ω_0 is the cyclic revolution frequency. For PF ring $\omega_0 = 2\pi\cdot 1.6MHz$. Then, g describes the vertical profile of the taper along the z axis, and w is the width of the taper.

We need a careful treatment of the transverse impedance, since it includes both the dipolar and the quadrupolar components [9]:

$$W_{y,tot}(y_1, y_2, z) = W_{y,dip}(z)\,y_1 + W_{y,quad}(z)\,y_2, \qquad (3)$$

ISBN: 978-3-95450-184-7 doi:10.18429/JACoW-IPAC2018-THPAK001

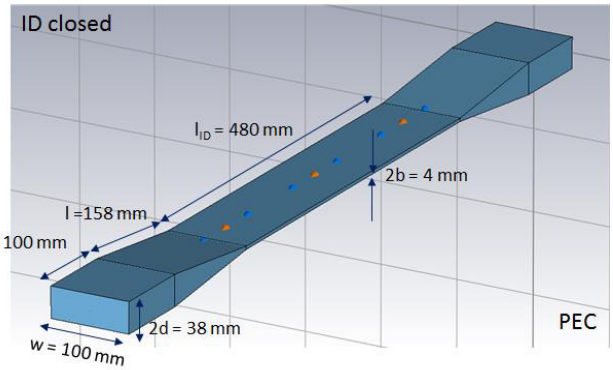

Figure 2: CST model of the IVU taper.

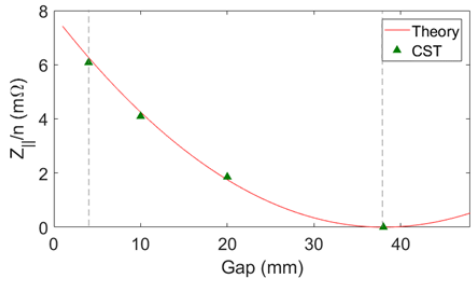

Figure 3: Normalized longitudinal impedance of the taper as a function of the gap (the width fixed to 100 mm) by theory (red line), and by simulations (green triangle).

where $W_{y,tot}(y_1, y_2, z)$ is a total wake received by the beam. In CST simulations they can be calculated by displacing the beam and the wake integration path separately [10]. According to Krinsky [11], theoretical formula for dipolar impedance is the following:

$$Z_{yD}(k) = -i\frac{Z_0}{2\pi b}\int_{-\infty}^{\infty}\frac{\xi^2}{\sinh^2\xi}\sum_{n=0}^{\infty}\delta_n\frac{H(k_n,k)+H(k_n,-k)}{2ik_n b}d\xi \quad (4)$$

$$P(p,k) = \int_{-\infty}^{\infty}\int_{-\infty}^{z_1} S'(z_1)S'(z_2)e^{i(p+k)(z_1-z_2)}dz_1dz_2, \quad (5)$$

where k is a perturbation wave number, $k_n b = \sqrt{(kb)^2 - \xi^2 - (\pi n)^2}$, and $S(z) = (a(z) - a_0)/a_0$ denotes a fractional deviation of the taper radius from the average one (a_0). For analytical estimation of the quadrupolar impedance, Stupakov's formula [8] is used:

$$Z_{yQ} = -i\frac{\pi Z_0}{4}\int_{-\infty}^{\infty}\frac{(g')^2}{g^2}G\left(\frac{g}{w}\right)dz, \quad (6)$$

with

$$G(x) = x^2\sum_{m=0}^{\infty}(2m+1) \times \operatorname{sech}^2\left((2m+1)\frac{\pi x}{2}\right)\tanh\left((2m+1)\frac{\pi x}{2}\right). \quad (7)$$

Each of dipolar and quadrupolar impedances produces vertical kick factors. In the case of Gaussian beam their relation could be expressed by the following:

$$k_y = \frac{\operatorname{Im} Z_y c}{2\sqrt{\pi}\sigma_z}. \quad (8)$$

Figures 4 and 5 give the comparison of the analytical Eqs. (4) – (5) and (6) – (7) with the CST simulation results for the dipolar and quadrupolar vertical kicks of the taper.

To sum up, the calculation of kick factors is most important since it provides additional coherent vertical tune shift. During machine measurements a tune shift could be detected. It includes both of dipolar and quadrupolar impacts.

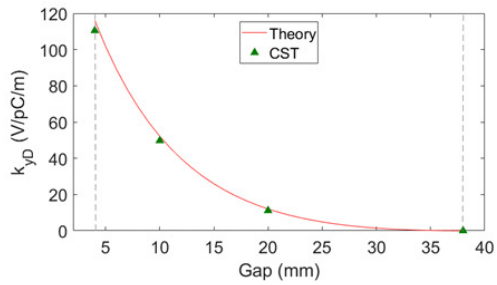

Figure 4: Dipolar vertical kick factor of the taper as a function of the gap (the width fixed to 100 mm) by theory (red line), and by simulations (green triangle).

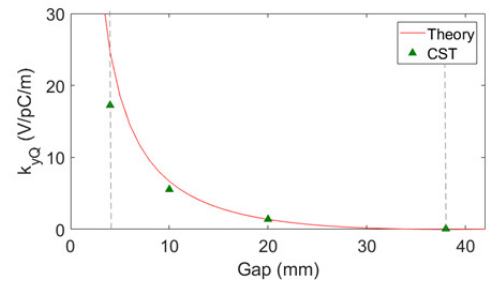

Figure 5: Quadrupolar vertical kick factor of the taper as a function of the gap (the width fixed to 100 mm) by theory (red line), and by simulations (green triangle).

Resistive-Wall Impedance of Undulator

By using the copper resistivity in CST, we can calculate the resistive-wall impedance of the undulator with the copper plate (the electric conductivity of Cu is $\sigma_c = 5.96\times10^7\, S/m$).

The vertical kick factor of the undulator plates was estimated using the following relation [12]:

$$k_{yR.W.} = \frac{cL}{8b^3}\sqrt{\frac{2Z_0 c}{\sigma_z\sigma_c}}\Gamma\left(\frac{5}{4}\right), \quad (9)$$

where L is a length of the undulator (L=480mm for PF IVU), and $\Gamma\left(\frac{5}{4}\right) = 0.9064$. The comparison of Eq. (9) with

ISBN: 978-3-95450-184-7 doi:10.18429/JACoW-IPAC2018-THPAK001

the CST simulation is given in Fig. 6. It demonstrates an excellent agreement between theory and simulations.

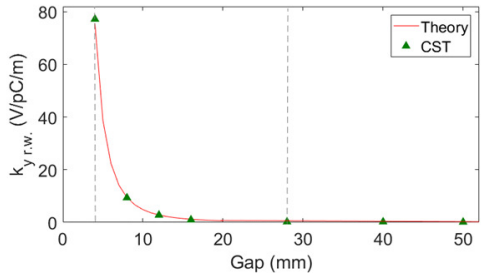

Figure 6: Resistive-wall vertical kick factor of the undulator (the width and the length are fixed to 100 mm and 480 mm, respectively) by theory (red line), and by simulations (green triangle).

Geometrical Impedance of Step Transition

The impact of the step transition is three orders less than other components and thus we ignore it in the following.

Total Transverse Impedance of the IVU

The total vertical kick factor due to 1 IVU including dipolar and quadrupolar kicks of the taper and resistive-wall kick of the undulator copper plates is summarized in Fig. 7. Table I provides more detailed information regarding the kick values.

An excellent agreement is seen between the theoretical predictions and the CST Studio simulations for PF IVU. Therefore, the new impedance evaluations of PF IVU are accurate enough in the framework of the theory and the simulation codes.

Before moving to the next section (tune shift measurement) some preparation work should be done. Namely, we need to evaluate an additional betatron tune shift ($\Delta\nu$) by 4 IVU at PF. We apply a well-known relation [13]:

$$\frac{\Delta\nu}{I_b} = -\frac{4\langle\beta\rangle k_y}{4\pi f_0 (E/e)}, \qquad (10)$$

where I_b is the bunch current, $f_0 = 1.6MHz$ is the revolution frequency of PF ring, and E is the beam energy (at PF $E = 2.5GeV$). With kick data shown in Table I, one can obtain $\Delta\nu / I_b = -9.713\times10^{-6} mA^{-1}$ as the simulation result, and $\Delta\nu / I_b = -10.39\times10^{-6} mA^{-1}$ as the analytical result. These are reference points for measurements.

Table 1: Vertical Kick Factors of PF IVU

Vertical kick factor per 1 IVU		CST PS	Theory
Taper vertical kick factor, V/pC/m	Dipolar	110.47	116.13
	Quadrupolar	16.64	24.61
Undulator vertical kick factor, V/pC/m	Dipolar	50.80	75.57
	Quadrupolar	26.40	
Total vertical kick factor, V/pC/m		204.31	216.31

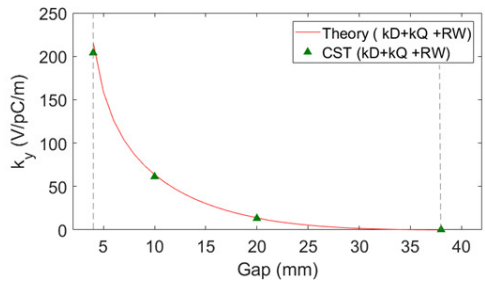

Figure 7: Total vertical kick factor of the IVU as a function of the gap (the width fixed to 100 mm) by theory (red line), and by simulations (green triangle).

MEASUREMENTS OF KICK FACTORS

We carried out tune shift measurements at PF based on the RF-KO (RF Knock Out) method [13]. The additional tune shift corresponds to a difference of the vertical tune shifts for ID open (gap=38mm) and ID closed (gap=4mm) cases. The results of the tune shift measurement are shown in Fig. 8. The data were measured manually about 20 times at each current value with a step of 0.5~1 mA. We obtain the tune shift $\Delta\nu / I_b = -11.7615\times10^{-6} \pm 1.4955\times10^{-6}$ (the average result of four measurements including a data fitting error). The measured tune shift is in very good agreements with both the theoretical prediction and the CST Studio simulation results.

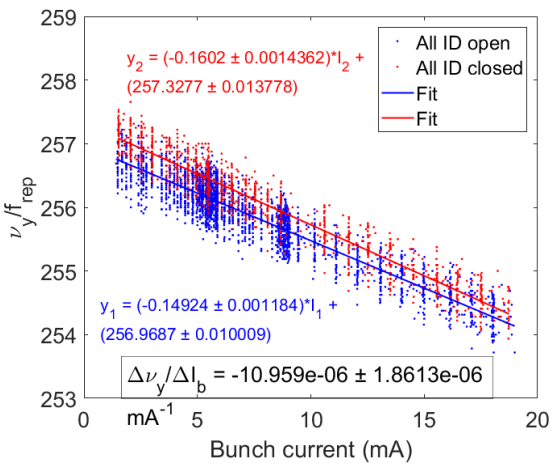

Figure 8: One of the measurement results of the additional tune shift due to the four IVU at PF.

Another method to measure a vertical kick of the IVU, called “the orbit bump”, was introduced in [14] and has been further developed in the works [15] – [16]. The orbit bump measurement is scheduled in this spring.

CONCLUSION

In summary, we have identified the major impedance contributors of PF IVU and successfully evaluated their impedance using the theoretical formulas, the CST Studio simulations and the measurements. The three evaluations show very good agreements. The present methods and procedures will greatly help the design of future IVU for further reduction of impedance.

ISBN: 978-3-95450-184-7 doi:10.18429/JACoW-IPAC2018-THPAK001

REFERENCES

[1] V. Smaluk *et al.*, "Coupling impedance of an in-vacuum undulator: Measurement, simulation, and analytical estimation.", *Phys. Rev. ST Accel. Beams*, vol. 17, p. 074402, Jul. 2014.

[2] E. Gjonaj *et al.*, "Computation of wakefields for an in-vacuum undulator at PETRA III", in *Proc., 4th Int. Particle Accelerator Conf. (IPAC 2013),* Shanghai, China, May, 2013, paper TUPWA008, pp. 1736-1738.

[3] F. Cullinan *et al.*, "Evaluation of In-Vacuum Wiggler Wakefield Impedances for SOLEIL and MAX IV", presented at the 22nd European Synchrotron Light Source Workshop (ESLS XXII), Grenoble, France, Nov. 2014.
http://www.esrf.eu/files/live/sites/www/files/events/conferences/2014/XXII%20ESLS/CULLINAN_wigglerimpedance.pdf

[4] T.F. Günzel, "Coherent and incoherent tune shifts deduced from impedance modelling in the ESRF-ring", in *Proc., 9th .8.124403 European Particle Accelerator Conf. (EPAC 2004),* Lucerne, Switzerland, July, 2004, paper WEPLT083, pp. 2044-2046.

[5] CST-Computer Simulation Technology, CST PARTICLE STUDIO, http://www.cst.com/Content/Products/PS/Overview.aspx.

[6] E. Belli *et al.*, arXiv:1609.03495.

[7] K. Bane, "Review of collective effects in low emittance rings", presented at the 2nd Topical Workshop on Instabilities, Impedance and Collective Effects (TWIICE2), Abingdon, UK, Feb. 2016.
https://indico.cern.ch/event/459623/contribu-tions/1131155/attachments/1224365/1791598/Bane_collective_ler.pdf

[8] G.V. Stupakov, Phys. Rev. ST Accel. Beams 10, 094401 (2007).

[9] B. Salvant, "Transverse single-bunch instabilities in the CERN SPS and LHC", presented at the Beam Physics for FAIR Workshop, Bastenhaus, Germany, Jul. 2010. https://indico.gsi.de/event/1031/

[10] C. Zannini, "Electromagnetic simulation of CERN accelerator components and experimental applications", Ph.D. thesis, Phys. Dept., Ecole Polytechnique F´ed´erale de Lausanne, Lausanne, Switzerland, 2013.

[11] S. Krinsky, Phys. Rev. ST Accel. Beams 8, 124403 (2005).

[12] A. Piwinski., "Impedance in lossy elliptical vacuum chambers", DESY, Hamburg, Germany, Report No. DESY-94-068, Apr. 1994.

[13] S. Sakanaka, T. Mitsuhashi, and T. Obina, Phys. Rev. ST Accel. Beams 8, 042801 (2005).

[14] V. Kiselev and V. Smaluk, "Measurement of local impedance by an orbit bump method," Nucl. Instrum. Methods A 525, 433 (2004).

[15] L Emery, G. Decker, and J. Galayda, in *Proc., 19th Particle Accelerator Conference (PAC2001)*, Chicago, USA, Aug. 2001, paper TPPH070, pp. 1823-1825.

[16] E. Karantzoulis, V. Smaluk, and L. Tosi, Phys. Rev. ST Accel. Beams 6, 030703 (2003).